The Dimethyl Ether−OCS Dimer: Rotational Spectrum, Structure, and Ab Initio Calculations

Josh J. Newby, Rebecca A. Peebles, and Sean A. Peebles*

Department of Chemistry, Eastern Illinois University, 600 Lincoln Avenue, Charleston, Illinois 61920

Received: May 28, 2004; In Final Form: July 7, 2004

The rotational spectra of the normal species and four isotopically substituted species of the dimethyl ether−OCS dimer have been measured by Fourier transform microwave spectroscopy, thereby allowing a structural determination of this weak complex. The normal isotopic species rotational constants are $A = 4069.4106(23)$ MHz, $B = 1431.7413(7)$ MHz, and $C = 1074.2925(5)$ MHz, and the experimental dipole moment components are $\mu_a = 1.3046(28)$ D, $\mu_b = 0.8134(37)$ D, with $\mu_{total} = 1.5374(30)$ D. Rotational constants, dipole moment components, and planar moments are all consistent with a geometry in which the OCS molecule is located in the heavy-atom plane of dimethyl ether, making an O···C−S angle of 96.5(2)°, and with an O···C separation of 2.916(3) Å. Ab initio calculations at the MP2/6-311++G(2d,2p) level reproduce the structure accurately, predicting rotational constants of $A = 4065$ MHz, $B = 1450$ MHz, and $C = 1083$ MHz.

Introduction

In recent years, a growing interest in the study of weak hydrogen bonding has been reflected in an increasing number of articles on the subject in the scientific literature. Reviews of the status of research in the field,[1] discussions of the true nature of the weak H-bonding interaction,[2,3] and even a dedicated book[4] on the subject appear in the literature. In the last 2−3 years, several high-resolution spectroscopic studies on dimers that exhibit weak C−H hydrogen bonds have been performed,[2,5,6] leading to structural data on these weak interactions in the gas phase, where there are no perturbations from solvent or lattice effects. In the past, there was considerable debate over whether C−H interactions could truly be classified as hydrogen bonds.[1] This uncertainty mainly arose because most of the early data on these interactions was obtained from crystal studies, and therefore, it was often unclear to what extent the constraints of the crystal lattice governed the intermolecular distances. The existence of weak hydrogen bonds of this variety is now accepted, and the increasing amount of gas-phase spectroscopic data should allow the C−H interaction to be further studied and quantified.

Early examples of high-resolution studies on systems containing C−H hydrogen bonds include complexes of oxirane with proton donors such as HF[7] and trifluoromethane.[2] The hydrogen atoms in oxirane have acidic properties because they are located on a carbon atom adjacent to the electronegative oxygen atom, and they can therefore form hydrogen bonds to proton acceptors on other species. The oxirane−trifluoromethane complex is particularly noteworthy because both one C−H···O bond (with oxirane acting as a proton acceptor) and two C−H···F−C bonds (with oxirane acting as a proton donor) are observed.[2]

An obvious extension to the study of oxirane complexes is the investigation of clusters involving dimethyl ether (DME). The location of the methyl groups next to the electronegative oxygen atom makes DME another good candidate for the formation of C−H hydrogen bonding interactions. In addition, dimethyl ether has two internal rotors and has received considerable attention as a prototypical double internal rotor system.[8−10] Because complexation is likely to influence the DME barrier to internal rotation, useful information on the strength of the interaction might be available from studies of any internal rotation splittings. Since the year 2000, the groups of Caminati and Alonso have characterized several weakly bound complexes of DME using Fourier transform microwave (FTMW) and free-jet absorption millimeter wave (FJ-AMM) techniques. Complexes studied to date include the DME dimer,[5] DME−HF,[6] and DME complexed with the rare gases Ne,[11] Ar,[12] Kr,[13] and Xe.[14] The DME dimer was determined to have a structure with C_s symmetry in which the formation of three C−H···O bonds appears to restrict the motion of three of the four methyl groups in the complex, considerably reducing the magnitude of the internal rotation splittings in the microwave spectrum. The fourth methyl group rotates more freely, and this motion does lead to some small spectral splittings. In DME−HF, the HF approaches the oxygen atom of DME (H atom first) along an axis that is about 40° to the C_2 axis of the DME[6] (rather than at the considerably larger angle of 70° observed in oxirane−HF[7]). The HF molecule in the DME−HF complex exhibited wide amplitude motions in which it tunneled from one side of the DME plane to the other, giving rise to inversion splittings in the spectrum. In addition, some fine structure due to the rotation of the methyl groups, ranging from 50 to 500 kHz in magnitude, was observed for some of the transitions in the DME−HF spectrum, allowing a calculation of the V_3 barrier.[6] In the DME−rare gas complexes,[11−14] only dispersion forces are present, and the rotation of the methyl groups appears to be completely damped, although there is again a tunneling motion associated with the rare gas atom moving from one side of the DME plane to the other.

The majority of previous experimental work has focused on complexes of DME with a proton donor, and few examples are to be found of DME complexed with a molecule that does not contain an acidic hydrogen atom. (One such example is DME−SO_2,[15] in which the molecular planes of the monomers line up approximately parallel, with the O−C bonds and the S═O bonds

* Corresponding author. E-mail: sapeebles@eiu.edu. Phone: (217) 581-2679. Fax: (217) 581-6613.

10.1021/jp0476747 CCC: $27.50
Published on Web 08/17/2004

eclipsing each other.) Given the lack of data for this type of system, it is of interest to investigate the nature of bonding of DME with molecules that do not possess acidic protons to donate to the oxygen atom of the ether. The DME−CO_2 complex, for example, has been previously studied in a combined IR (in liquid Ar) and ab initio investigation,[16] and the complex was proposed to have a structure in which the CO_2 lies perpendicular to the C_2 axis of DME, giving a complex with C_{2v} symmetry and an ab initio C···O bond length of 2.812 Å. (Preliminary results from an investigation of the microwave spectrum of DME−CO_2 in our laboratory have confirmed the C_{2v} structure of the complex, but indicate a C···O distance nearer to 2.711(5) Å.[17]) Some evidence of blue shifts in the C−H stretching vibrations was seen in the calculated and observed vibrational frequencies in the IR study of DME−CO_2, and this might be interpreted as an indication of C−H hydrogen bonding interactions.[16] Substitution of the CO_2 with a polar carbonyl sulfide (OCS) molecule might provide another opportunity to observe intermolecular C−H···O interactions. Alignment of the OCS approximately perpendicular to the C_2 axis of DME (in the same fashion as for the DME−CO_2 complex) will make the methyl groups inequivalent and will likely appreciably influence their barriers to internal rotation; it should be informative to determine whether torsional splittings are observable. A second possibility for the structure of DME−OCS is suggested by direct comparison with the H_2O−OCS dimer. In this complex, the S atom of OCS interacts with the O atom of H_2O to give a linear configuration of heavy atoms.[18] The current paper presents the assignment of the rotational spectra of five isotopomers of the DME−OCS weakly bound complex and a determination of the structure of this dimer from the experimental moment of inertia data and by ab initio calculations.

Experimental Section

The rotational spectra of five isotopomers of the DME−OCS weakly bound dimer were measured between 6 and 15 GHz using a Balle−Flygare-type Fourier transform microwave spectrometer[19] based upon the University of Kiel design.[20] Samples comprising approximately 1.5% dimethyl ether (99+%, Sigma-Aldrich), 1.5% carbonyl sulfide (97.5+%, Sigma-Aldrich), and 97% first-run He/Ne (17.5%/82.5%) contained in a 2 L glass sample bulb were expanded through a 0.8 mm diameter General Valve series 9 solenoid valve operating at 10 Hz. Backing pressures of the He/Ne carrier gas were kept at about 1.2−1.8 atm for the best signal intensity. The most intense spectral transitions belonging to this weak complex were observed to have a signal-to-noise ratio of about 40 in 100 gas pulses. Frequency measurements were reproducible to 4 kHz, and the transitions typically had a fwhm of 30 kHz. Initial assignment of the spectrum was made by identification of the Stark effects of the $3_{13}-2_{12}$ and $2_{12}-1_{01}$ transitions, the Stark shifts having been predicted using the lowest-energy structure provided by an MP2 ab initio optimization (to be described in section IV of Results and Discussion). Stark effect measurements were carried out by the application of voltages up to ±6 kV to a pair of parallel steel mesh plates (separated by approximately 30 cm) located within the Fabry−Pérot cavity of the spectrometer. Daily calibration of the electric field was carried out with the $J = 1 \leftarrow 0$ transition of OCS, assuming a dipole moment of 0.715 21 D.[21] Because of the high price of isotopically enriched samples of OCS and the lack of commercially available ^{13}C-substituted DME, the rotational spectra of all isotopomers were measured in natural abundance. The weakest ^{13}C species required averaging for 20 000 gas pulses to achieve a respectable signal-to-noise ratio; nevertheless, the signal intensity was still relatively poor (the weakest of these signals was at the detection limit of our instrument and was comparable in signal power to background noise levels). In light of the considerably lower intensity for the transitions belonging to the isotopic species, we assign a higher uncertainty of 8 kHz to these transition frequencies.

During the search for the spectrum of the DME−OCS complex, the $J = 2 \leftarrow 1$ a-type transitions (K_a's = 0 and 1) belonging to the DME−CO_2 complex were also located. These transitions were observed in reasonable intensity (a signal-to-noise ratio of about 30 in 100 gas pulses), presumably due to a CO_2 impurity in the OCS. Replacement of the OCS in the sample by CO_2 led to an order of magnitude increase in the signal-to-noise ratio of the transitions, confirming the carrier of the spectrum. Details of the analysis of the DME−CO_2 spectrum will be presented in a forthcoming paper.[17]

Results and Discussion

I. Spectra. a- and b-type rotational transitions were observed for all isotopic species, with the more intense a-type transitions requiring an optimum microwave pulse length that was of shorter duration than that of the b-type lines, suggesting a slightly larger a-dipole moment component. Attempts to locate c-type transitions at their predicted frequencies were not successful, although an absence of c-type lines is consistent with the plane of symmetry resulting from analysis of the structural data (see section II, Structure). No obvious indications of internal rotation splittings in any of our isotopic spectra were observed. It should be noted that, in the case of the DME dimer,[5] the splittings arising from internal rotation of the single free methyl group that was not involved in hydrogen bonding interactions were typically 20 kHz or less (although two transitions were split by 58 and 95 kHz); the smallest splitting is a little less than the fwhm in our current experiments. Analysis of the splittings in the DME dimer yielded a V_3 barrier estimate of 2.2 kcal/mol[5] (while several studies determine the monomer value to be around 2.6 kcal/mol).[8−10] The lack of observed splittings in the current work indicates that the barrier to internal rotation in this complex is changed relative to the DME monomer, the spectrum of which contains splittings of the order of a few megahertz. Of course, in the DME−OCS dimer, we expect the two methyl groups to be inequivalent, so the nature of the internal rotation splittings may be significantly different than in the monomer. In the course of the extended averaging required to measure the ^{13}C lines, some additional transitions of similar intensity were found, although no discernible patterns were observed that suggested any internal rotation splittings. It is proposed that these additional lines may arise from other isomers of the dimer or from trimeric and higher clusters and that any internal rotation splittings are smaller than the resolution of the current work.

The 33 measured transitions for the normal isotopomer are listed in Table 1, along with the residuals from a least-squares fit of the transition frequencies to a Watson *A*-reduction Hamiltonian in the I^r representation[22] (using the *SPFIT* program of Herb Pickett[23]). Analysis of the isotopic species' spectra (DME−OC^{34}S, two unique ^{13}C-substituted-DME−OCS species, and DME−O^{13}CS) was carried out in the same manner except for the need to fix some of the centrifugal distortion constants to the values obtained for the normal isotopic species. This was a result of the smaller data sets arising from the lower transition intensities of the isotopic species, but it did not noticeably affect the quality of the fits. The spectroscopic constants for all of the isotopic species are listed in Table 2.

TABLE 1: Rotational Transitions for the Normal Isotopomer of Dimethyl Ether−OCS

$J'_{K_aK_c}$	$J''_{K_aK_c}$	ν/MHz	$\Delta\nu^a$/MHz
2_{12}	1_{01}	7 292.2626	−0.0021
2_{20}	2_{11}	7 946.9008	0.0006
2_{21}	2_{12}	8 985.2489	−0.0015
2_{21}	1_{10}	13 282.4088	−0.0017
2_{20}	1_{11}	13 673.7603	0.0049
3_{13}	2_{12}	6 961.5304	−0.0007
3_{03}	2_{02}	7 384.2317	0.0007
3_{22}	2_{21}	7 517.9001	−0.0008
3_{21}	3_{12}	7 566.7691	0.0025
3_{21}	2_{20}	7 651.5643	−0.0022
3_{12}	2_{11}	8 031.6989	−0.0012
3_{13}	2_{02}	9 275.7036	−0.0003
3_{22}	3_{13}	9 541.6182	−0.0020
4_{22}	4_{13}	7 221.8795	−0.0009
4_{04}	3_{13}	7 810.0209	−0.0010
4_{14}	3_{13}	9 246.7638	−0.0020
4_{04}	3_{03}	9 701.4954	0.0007
4_{23}	3_{22}	9 997.2442	0.0048
4_{32}	3_{31}	10 085.8163	0.0043
4_{23}	4_{14}	10 292.0972	0.0034
4_{22}	3_{21}	10 319.2899	−0.0046
4_{14}	3_{03}	11 138.2401	0.0015
5_{14}	5_{05}	6 321.5531	0.0024
5_{23}	5_{14}	7 024.8376	−0.0006
5_{05}	4_{14}	10 490.5096	0.0031
5_{24}	5_{15}	11 238.8615	−0.0048
5_{15}	4_{14}	11 507.2178	−0.0013
5_{05}	4_{04}	11 927.2505	0.0000
5_{15}	4_{04}	12 943.9616	−0.0015
5_{14}	4_{13}	13 252.2079	−0.0003
6_{06}	5_{15}	13 066.6488	−0.0019
6_{16}	5_{15}	13 742.5566	0.0010
6_{06}	5_{05}	14 083.3637	0.0004

[a] $\Delta\nu = \nu_{obs} - \nu_{calc}$ where ν_{calc} is computed from the constants in Table 2.

II. Structure. Location of the isotopic spectra was aided by isotopic shifts calculated from the lowest-energy MP2-optimized structure of the complex. This calculation predicted a heavy-atom planar arrangement of the DME and OCS molecules, with the OCS molecule forming an O···C−S angle of about 97.7° (see Figure 1). Transitions were located within 2−4 MHz of the predicted frequencies, emphasizing the accuracy of the theoretical predictions.

Further corroboration of this proposed structure was available from an inspection of second-moment data for the various isotopomers of the complex. The second moment, P_{cc}, depends on the *c*-principal-axis coordinates of the atoms according to

$$P_{cc} = \sum_i m_i c_i^2 \qquad (1)$$

where m_i is the mass of atom i and c_i is the *c*-coordinate of the atom. In the case of a heavy-atom planar arrangement for this dimer, we would expect the P_{cc} values for all isotopomers to be similar to each other as well as close in magnitude to the P_{cc} value of the DME monomer. It can be seen from the bottom row of Table 2 that the P_{cc} value of the dimer in all species is close to the P_{cc} second moment of the DME monomer[24] (3.207 amu Å^2). The small difference between monomer and dimer values is due to vibrational contamination from low-frequency van der Waals modes within the complex. The insensitivity of P_{cc} to the isotopic substitutions (which all take place in the *ab*-plane) proves convincingly that the OCS molecule lies in the heavy-atom plane of DME.

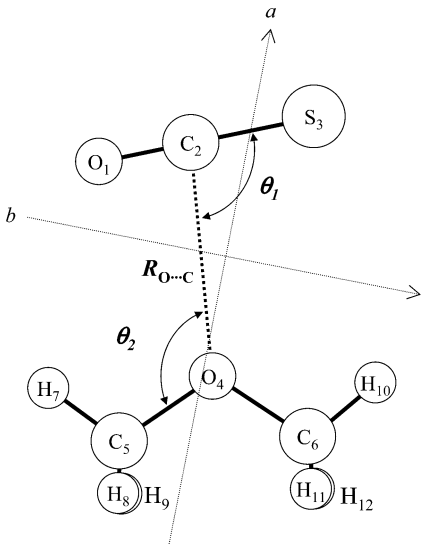

Figure 1. Structure of the DME−OCS dimer showing the atom numbering and the three parameters required to describe the structure. Atoms numbered H_9 and H_{12} are the hydrogen atoms behind H_8 and H_{11}, respectively.

The 15 moments of inertia obtained from fitting the measured transitions of the five isotopomers enabled a least-squares fit of these moments to the three structural parameters that are required to describe the dimer geometry (the O···C distance, the O_4···C_2−S_3 angle, θ_1, and the C_2···O_4−C_5 angle, θ_2; see

TABLE 2: Spectroscopic Constants for Five Isotopomers of the DME−OCS Dimer[a,b]

parameter	normal	$^{13}C_2$	$^{34}S_3$	$^{13}C_5$	$^{13}C_6$
A/MHz	4069.410 6(23)	4055.9472(40)	4030.558 67(74)	4044.8369(53)	4006.5217(42)
B/MHz	1431.741 32(71)	1424.6641(19)	1402.800 82(80)	1407.7131(21)	1415.5489(19)
C/MHz	1074.292 50(50)	1069.3687(10)	1055.260 48(49)	1059.0462(12)	1060.7935(11)
Δ_J/kHz	1.897(10)	1.877(23)	1.810(12)	1.787(24)	1.808(24)
Δ_{JK}/kHz	−181(58)	[−181]	[−181]	[−181]	[−181]
Δ_K/kHz	4.44(45)	[4.44]	[4.44]	[4.44]	[4.44]
δ_J/kHz	0.516 7(67)	0.477(22)	0.474 5(85)	0.482(26)	0.462(23)
δ_K/kHz	3.68(21)	[3.68]	[3.68]	[3.68]	[3.68]
N^c	33	16	20	12	14
$\Delta\nu_{rms}$/kHz[d]	2.34	3.84	3.41	3.88	3.75
P_{aa}/amu Å^2 [e]	349.611 0(2)	351.3647(4)	356.895 7(2)	355.6325(5)	353.6484(4)
P_{bb}/amu Å^2	120.818 7(1)	121.2310(1)	122.018 3(1)	121.5696(1)	122.7677(1)
P_{cc}/amu Å^2	3.3711 0(1)	3.3709(1)	3.368 6(1)	3.3747(1)	3.3715(1)

[a] Atom numbering is shown in Figure 1. [b] The centrifugal distortion constants (Δ_{JK}, Δ_K, δ_K) were fixed for all isotopomers at the values obtained from the fit of the normal isotopomer transitions. [c] *N* is the number of fitted transitions. [d] $\Delta\nu_{rms} = [\sum(\nu_{obs} - \nu_{calc})^2/N]^{1/2}$. [e] Second moments: see the text for discussion and definition.

TABLE 3: Structural Parameters Obtained from Fitting Various Combinations of Moments of Inertia for All Isotopic Species[a]

parameters	fit I_a, I_b	fit I_a, I_c	fit I_b, I_c	fit I_a, I_b, I_c	best[b]	ab initio[c]
$R_{O\cdots C}$/Å	2.919 2(4)	2.917 3(4)	2.914 3(3)	2.9170(12)	2.916(3)	2.864
θ_1/deg	96.38(2)	96.37(2)	96.71(2)	96.49(6)	96.5(2)	97.7
θ_2/deg	120.0(3)	119.9(3)	119.95(19)	119.9(8)	119.9(1)	120.1
ΔI_{rms}[d]	0.029 69	0.026 51	0.029 08	0.1295		
R_{cm}[e]	3.565 6(5)	3.563 8(4)	3.563 8(4)	3.5644(15)	3.565(1)	3.536

[a] Structural parameters are defined in Figure 1. [b] Estimated best values from the various inertial fit values. [c] Ab initio parameters are obtained from the MP2/6-311++G(2d,2p) optimization. [d] ΔI_{rms} is the root-mean-square deviation of the least-squares fit, defined by $\Delta I_{rms} = ((\sum(I_{obsd} - I_{calcd})^2/N))^{1/2}$ where N is the number of moments fitted. [e] R_{cm} is the center of mass separation, calculated from the principal axis coordinates.

Figure 1 for atom numbering); this fit was carried out using the *STRFITQ* program of Schwendeman.[25] The geometries of both the DME[24] and OCS[26] monomers were held fixed at their literature values during the fitting process. Several variations of the fitting process were carried out, including separate fits that combined pairs of moments of inertia ((I_a, I_b), (I_b, I_c), and (I_a, I_c)) for all isotopic species, and also a fit including all three of the moments (I_a, I_b, and I_c) for all species. The parameters derived from the different inertial fits were very similar and are shown in Table 3, along with an estimation of the best value and uncertainty for each of the fitted parameters. The O···O and O···S distances (measured from the oxygen atom of the DME to the O or S atom of the OCS) derived from the fitted structure are 3.01 and 3.46 Å, respectively. It is interesting to note that this difference in distances accurately reflects the difference in the Pauling van der Waals radii of the O and S atoms (O = 1.4 Å, S = 1.85 Å).[27] Hence, the tilt of the OCS can be largely explained by the different sizes of the O and S atoms of the OCS molecule. The C—H···O angle determined from the inertial fit structure is around 115°, while the C—H···O distance is 2.90 Å, approximately 0.3 Å longer than the classical H···O van der Waals separation of 2.6 Å. This C—H···O contact is strongly bent, so it is unclear whether the electrostatic energy contributions are particularly attractive in this orientation. Because it has been previously shown that H···O contacts show a continuous transition from stronger to weaker and finally to nonbonding interactions,[28] it is difficult to quantify the importance of the C—H···O contact in the DME−OCS complex.

Single isotopic substitution data allow an independent verification of the inertial fit results by providing principal axis coordinates for each of the substituted atoms. The three carbon atoms (the C atom in OCS and both of the C atoms in DME) and the S atom of OCS were all singly substituted, and using the equations of Kraitchman,[29] it was possible to determine the magnitude of the principal axis coordinates for those atoms. The coordinates resulting from the Kraitchman calculations are given in Table 4, along with the principal axis coordinates for the same atoms obtained from the inertial fit. It can be seen that the two sets of coordinates are in reasonably good agreement. The C═S bond distance in OCS, determined from the Kraitchman coordinates, is 1.5600(1) Å (compared to the literature value[26] of 1.5651 Å), and the C···C distance between the two carbon atoms in the DME monomer is determined to be 2.3372(2) Å (compared to the literature value[24] of 2.332 Å). These parameters are both within 0.5% of the literature values, providing a degree of confidence in our inertial fit results and providing justification of the assumption that the monomer geometries remain unchanged in the dimer.

III. Dipole Moment. The dipole moment of the DME−OCS complex was determined from measurements of second-order Stark shifts for 13 M_J components selected from five rotational transitions. A least-squares fit of measured $\Delta\nu/E^2$ values to calculated Stark coefficients (obtained from perturbation theory calculations using the rotational constants given in Table 2) allowed determination of the μ_a and μ_b dipole components. The μ_c component was held at zero in the fitting process due to the existence of an *ab*-symmetry plane. Attempts to fit this component gave unphysical values for μ_c^2 of −0.0012 D^2 and no variation in the values of the other two components. Measured Stark shifts were all less than 1 MHz, and no deviations from a second-order Stark effect were noted at the applied voltages of up to ±6 kV. Calculated and observed Stark coefficients, in addition to the derived dipole moment components, are listed in Table 5. The observed transition intensities are consistent with the experimental dipole moment components of μ_a = 1.3046(28) D and μ_b = 0.8134(37) D (μ_{total} = 1.5374(30) D). Using previously tabulated dipole moments for OCS[21] (μ_{total} = 0.715 21 D) and DME[30] (μ_{total} = 1.31 D) and our inertial fit structure, the projections of the dipole moments in the principal axis coordinate system can be calculated,

TABLE 4: Principal Axis Coordinates (in Å) for the Substituted Heavy Atoms in the DME−OCS Dimer Resulting from a Least-Squares Fit of the Moments of Inertia of Five Isotopomers[a,b]

atom	*a*	*b*	*c*
C_2	1.3438	−0.6558	0.0000
	[1.3271]	[0.6466]	[0.0000]
S_3	1.9247	0.7975	0.0000
	[1.9236]	[0.7949]	[0.0000]
C_5	−2.4709	−0.8791	0.0000
	[2.4573]	[0.8806]	[0.0605]
C_6	−2.0257	1.4100	0.0000
	[2.0068]	[1.4126]	[0.0192]

[a] The values in brackets are the absolute values of the Kraitchman substitution coordinates.The projected uncertainty in the values of the Kraitchman substitution coordinates is better than ±0.0001 Å. [b] See Figure 1 for atom numbering.

TABLE 5: Observed and Calculated Stark Coefficients and the Derived Dipole Moment Components for DME−OCS[a]

transition	$\lvert M\rvert$	$\Delta\nu/E^2$ obsd (10^{-6} MHz/V^2 cm^{-2})	$\Delta\nu/E^2$ calcd (10^{-6} MHz/V^2 cm^{-2})	% difference
$2_{12}-1_{01}$	0	−25.31	−25.63	−1.3
	1	23.48	23.46	0.1
$3_{13}-2_{12}$	0	−2.508	−2.433	3.0
	1	10.79	10.33	4.3
	2	48.68	48.62	0.1
$3_{03}-2_{02}$	0	−6.001	−5.801	3.3
	1	0.5292	0.5642	−6.6
	2	19.73	19.66	0.4
$3_{13}-2_{02}$	0	−9.181	−8.956	2.5
	1	−2.646	−2.509	5.2
	2	16.86	16.83	0.2
$4_{04}-3_{03}$[b]	2	4.255	4.345	−2.1
	3	12.08	12.51	−3.6

[a] μ_a = 1.3046(28) D; μ_b = 0.8134(37) D; μ_{total} = 1.5374(30) D. [b] The M = 0 and M = 1 components of the $4_{04}-3_{03}$ transition had very small Stark shifts and were not well resolved at voltages up to ±4 kV; hence, these components are not included in the dipole moment fit.

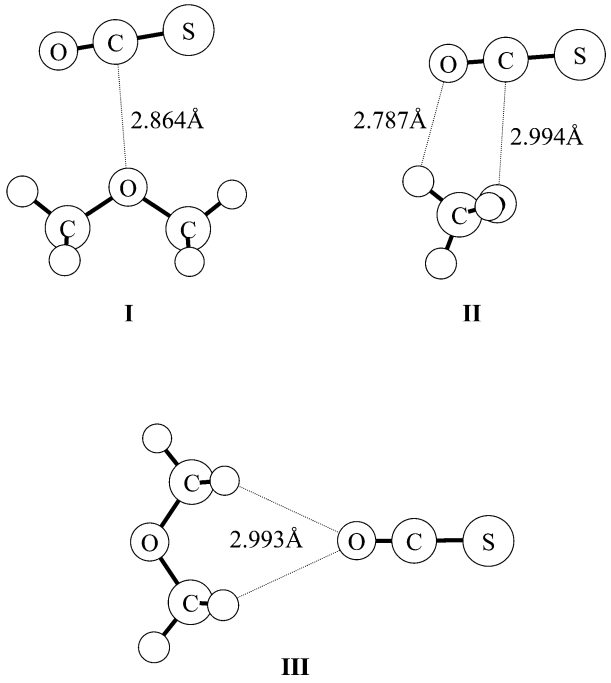

Figure 2. Three lowest-energy structures of the DME−OCS dimer obtained from the MP2/6-311++G(2d,2p) ab initio optimizations.

allowing for a comparison with the experimentally determined dipole moment components. This gives projected dipole components of $\mu_a = 1.02$ D and $\mu_b = 0.91$ D (with a μ_{total} of 1.37 D), in relatively good agreement with (but smaller than) the experimental values. Clearly, there are some induced dipole contributions, which lead to an increase of nearly 0.3 D in μ_a compared to the monomer projections. The experimental dipole moment components are also in good agreement with the predictions from the ab initio calculations (see section IV).

IV. Ab Initio Calculations. Ab initio optimizations were carried out on numerous possible structures for the DME−OCS dimer at various levels, including HF/6-31G and frozen core, second-order Møller−Plesset perturbation theory, MP2(FC), employing both 6-311+G(d,p) and 6-311++G(2d,2p) basis sets. All structure optimizations were performed using *Gaussian 98W*,[31] while vibrational frequency calculations at the highest level of computation were carried out with *Gaussian 98*[32] on a Tru64 Unix workstation. All basis sets used were the standard, unmodified basis sets provided in the Gaussian libraries.[31,32] Structure optimizations were carried out without any counterpoise (CP) corrections to the potential energy surface,[33] although basis set superposition error (BSSE) corrections were included in the interaction energy calculations using the CP correction procedure of Boys and Bernardi.[34] The optimizations were used to provide energetic stability information to establish the lowest-energy structure. The low-level HF calculations returned six possible geometries starting from numerous initial orientations (both chemically reasonable and unreasonable). These six structures were further reduced to three true minima when MP2/6-311+G(d,p) optimizations and vibrational frequency calculations were performed. The lowest-energy structures were then subjected to MP2 optimizations using the considerably larger 6-311++G(2d,2p) basis set (a total of 230 basis functions). The three lowest-energy structures (I−III) are shown in Figure 2, with the predicted rotational constants, dipole moment components, total energies, and computed interaction energies for the three structures listed in Table 6. Structure I resembles the experimentally determined geometry. Structure II places the OCS in the σ_v plane that bisects the C−O−C angle of the DME,

TABLE 6: Rotational Constants, Dipole Components, MP2 Total Energies, and Interaction Energies for the Three Lowest-Energy Optimized Structures of the DME−OCS Dimer[a]

	spectroscopic parameters	calculated energies	
		energy type	value
		Structure I[b]	
A/MHz	4065	MP2 energy/E_h[c]	−665.482 055
B/MHz	1450	ΔE/kJ mol^{-1} [d]	−14.1
C/MHz	1083	ΔE_{BSSE}/kJ mol^{-1} [e]	−9.3
μ_a/D	1.60		
μ_b/D	0.63		
		Structure II	
A/MHz	4307	MP2 energy/E_h	−665.482 034
B/MHz	1342	ΔE/kJ mol^{-1}	−13.9
C/MHz	1262	ΔE_{BSSE}/kJ mol^{-1}	−8.4
μ_a/D	0.79		
μ_b/D	0.25		
		Structure III	
A/MHz	10138	MP2 energy/E_h	−665.479 216
B/MHz	635	ΔE/kJ mol^{-1}	−6.4
C/MHz	603	ΔE_{BSSE}/kJ mol^{-1}	−2.7
μ_a/D	2.39		

[a] The three structures are pictured in Figure 2. [b] Structure I is the minimum energy configuration that most closely resembles the experimentally observed structure. [c] Total electronic energy. [d] Interaction energy, $\Delta E = E_{DME-OCS\ dimer} - E_{DME} - E_{OCS}$. [e] ΔE_{BSSE} is the BSSE corrected interaction energy (CP method).

and the O atom of OCS interacts with the methyl group hydrogen atoms. Structure III places the OCS in the heavy-atom plane of the DME with the O end of the OCS molecule interacting with the methyl group hydrogen atoms to give a structure with C_{2v} symmetry. The interaction energies in Table 6 are computed both with and without basis set superposition error (BSSE) corrections; BSSE corrections were calculated using the standard counterpoise correction procedure.[34,35] Structure I is the lowest in energy and has the largest interaction energy (−14.1 kJ mol^{-1}), although this value decreases in magnitude by about a third to −9.3 kJ mol^{-1} when BSSE corrections are taken into account. Structure II is the next most stable with an interaction energy (−13.9 kJ mol^{-1}) which is only 0.2 kJ mol^{-1} smaller than that of structure I; however, when BSSE corrections are included, this interaction energy is reduced to −8.4 kJ mol^{-1}, making the difference in stability between I and II greater. Structure III is the least stable, with an interaction energy of −6.4 kJ mol^{-1} (decreasing to less than half that value, −2.7 kJ mol^{-1}, with BSSE corrections). Zero point energy (ZPE) corrections have not been explicitly evaluated in the present work but are similar for both basis sets and are not expected to change the relative stabilities of the three structures. Estimations of ZPE corrections for the larger basis set suggest that the energy difference between I and II will be decreased while that between II and III will be increased slightly upon their inclusion. The complicated dependence of the potential energy surface, the ZPE, and, hence, the optimized structure of the complex, on BSSE[36] was not considered in this study. It should be further noted that structure II gives rise to one negative vibrational frequency at the MP2/6-311++G(2d,2p) level, in contrast to all positive frequencies at the MP2/6-311+G(d,p) level. A detailed analysis of the possible causes for this difference is beyond the scope of this work. The lack of consideration of the influence of the BSSE effects on the flat potential energy surface for this dimer, as well as the use of convergence thresholds in the optimization that are not sufficiently rigorous, may be possibilities for the cause of this behavior.

It was evident upon assignment of the spectrum that the predicted and observed rotational constants were very similar, suggesting that the predicted structure was a reasonably close approximation to the true structure. The lowest-energy configuration obtained from the ab initio calculations (structure I) is consistent with the structure obtained from fitting the spectral data. Isotopic shifts calculated from a slightly modified structure (in which the $R_{O\cdots C}$ distance was adjusted to agree better with the experimental rotational constants) were used to locate rotational transitions belonging to the isotopic species to within 4 MHz of the predictions. The structural parameters derived from the highest level MP2/6-311++G(2d,2p) calculation are listed in the last column of Table 3. It can be seen that the parameters from the MP2 calculation are in good agreement with the parameters obtained from the experimental determination, although the $R_{O\cdots C}$ distance is slightly underestimated in the ab initio calculation. Previous studies have indicated that fragment relaxation corrections in BSSE calculations on hydrogen-bonded systems[16,37] tend to result in slightly longer bond lengths, and better agreement might be obtained for the present species if these factors were fully considered; however, for our purposes of locating the lowest-energy configuration and of using the calculations as a tool to facilitate the spectral assignment, the present calculations provide more than satisfactory agreement.

A brief inspection of the computed vibrational frequencies in the region of the methyl group C−H stretch for the monomer and dimer shows no clear trend upon complex formation. In the DME−CO_2 study, some clear blue shifts were evident for the ν_1 and ν_{12} vibrational modes.[38] A comparison of the frequencies obtained in the current work using the MP2/6-311+G(d,p) and MP2/6-311++G(2d,2p) levels indicates a sensitivity to the basis set, and no conclusions can be drawn regarding possible C−H···O interactions. As a result, it would appear that ab initio calculations at an even higher level would be necessary to discern the true nature of the bonding and vibrational frequency shifts, as well as to show definitively whether any sort of C−H interaction is taking place.

Conclusions

The present work has described a determination of the structure of the DME−OCS dimer in the gas phase. The structure is similar to that proposed for DME−CO_2,[16,17] with the OCS monomer located in the heavy atom plane of the DME and aligned approximately perpendicular to its C_2 axis, with the O atom of OCS tilted toward the DME. The intermolecular O···C bond length in the OCS complex is found experimentally to be 2.916(3) Å and is similar to the ab initio estimate of the O···C bond length of 2.812 Å in the DME−CO_2 complex;[16] however, it is slightly more than 0.2 Å longer than the value of 2.711(5) Å determined by recent microwave measurements of DME−CO_2 in this laboratory.[17]

The ab initio optimizations predicted a lowest-energy structure that was in very good agreement with the experimentally determined rotational constants and dipole moment components. This theoretical structure was very useful both in the initial assignment of the spectrum and in the subsequent location of the isotopic species spectra. Internal rotation splittings were not resolved, apparently indicating that the motion of the DME methyl groups is considerably reduced relative to free DME monomer. Presumably, the interaction of the in-plane hydrogen atoms of the methyl groups with the OCS molecule restricts the motion of the methyl rotors in the DME.

Acknowledgment. Acknowledgment is made to the donors of the American Chemical Society Petroleum Research Fund for support of this research (PRF Grant 39752-GB6). The authors express their gratitude to Jim Wentz of Computer Electronics Electrical Services in the School of Chemical Sciences, University of Illinois Urbana Champaign, for his expertise and persistence in dealing with the problems arising from fitting the connectors for the high-voltage power supplies. The authors also thank Roy Wentz of the Department of Chemistry at the University of Michigan for constructing the high-vacuum line which was used for the preparation of the samples in this work.

Supporting Information Available: Tables of measured transition frequencies for the four isotopic species. This material is available free of charge via the Internet at http://pubs.acs.org.

References and Notes

(1) See for example: Jeffrey, G. A. *J. Mol. Struct.* **1999**, *485−486*, 293 and references therein.
(2) Alonso, J. L.; Antolínez, S.; Blanco, S.; Lessari, A.; López, J. C.; Caminati, W. *J. Am. Chem. Soc.* **2004**, *126*, 3244.
(3) Steiner, T.; Desiraju, G. R. *Chem. Commun.* **1998**, 891.
(4) The weak hydrogen bond in structural chemistry and biology, *International Union of Crystallography*; Desiraju, G. R., Steiner, T., Eds.; Oxford University Press: New York, 1999.
(5) Tatamitani, Y.; Bingxin, L.; Shimada, J.; Ogata, T.; Ottaviani, P.; Maris, A.; Caminati, W.; Alonso, J. L. *J. Am. Chem. Soc.* **2002**, *124*, 2739.
(6) Ottaviani, P.; Caminati, W.; Velino, B.; Blanco, S.; Lesarri, A.; Lopez, J. C.; Alonso, J. L. *ChemPhysChem* **2004**, *5*, 336.
(7) Legon, A. C.; Wallwork, A. L.; Millen, D. J. *Chem. Phys. Lett.* **1991**, *178*, 279.
(8) Hayashi, M.; Imachi, M. *Chem. Lett.* **1975**, 1249.
(9) Durig, J. R.; Li, Y. S.; Groner, P. *J. Mol. Spectrosc.* **1976**, *62*, 159.
(10) Niide, Y.; Hayashi, M. *J. Mol. Spectrosc.* **2004**, *223*, 152.
(11) Maris, A.; Caminati, W. *J. Chem. Phys.* **2003**, *118*, 1649.
(12) Ottaviani, P.; Maris, A.; Caminati, W.; Tatamitani, Y.; Suzuki, Y.; Ogata, T.; Alonso, J. L. *Chem. Phys. Lett.* **2002**, *361*, 341.
(13) Velino, B.; Melandri, S.; Caminati, W. *J. Phys. Chem. A* **2004**, *108*, 4224.
(14) Favero, L. B.; Velino, B.; Millemaggi, A.; Caminati, W. *ChemPhysChem* **2003**, *4*, 881.
(15) Oh, J. J.; Hillig, K. W., II; Kuczkowski, R. L. *Inorg. Chem.* **1991**, *30*, 4583.
(16) Van Ginderen, P.; Herrebout, W. A.; van der Veken, B. J. *J. Phys. Chem. A* **2003**, *107*, 5391.
(17) Newby, J. J.; Peebles, R. A.; Peebles, S. A. *J. Phys. Chem. A*, submitted for publication, 2004.
(18) Ogata, T. Personal communications, 2003.
(19) Balle, T. J.; Flygare, W. H. *Rev. Sci. Instrum.* **1981**, *52*, 33.
(20) Grabow, J.-U. Ph.D. Thesis, University of Kiel, 1992.
(21) Muenter, J. S. *J. Chem. Phys.* **1968**, *48*, 4544.
(22) Watson, J. K. G. *J. Chem. Phys.* **1967**, *46*, 1935.
(23) Pickett, H. M. *J. Mol. Spectrosc.* **1991**, *148*, 371.
(24) Niide, Y.; Hayashi, M. *J. Mol. Spectrosc.* **2003**, *220*, 65.
(25) Schwendeman, R. H. In *Critical Evaluation of Chemical and Physical Structural Information*; Lide, D. R., Paul, M. A., Eds.; National Academy of Sciences: Washington, DC, 1974.
(26) Harmony, M. D.; Laurie, V. W.; Kuczkowski, R. L.; Schwendeman, R. H.; Ramsay, D. A.; Lovas, F. J.; Lafferty, W. J.; Maki, A. J. *J. Phys. Chem. Ref. Data* **1979**, *8*, 619.
(27) Pauling, L. *College Chemistry*, 3rd ed.; W. H. Freeman and Company: San Francisco, 1964; p 290.
(28) Steiner, T.; Saenger, W. *J. Am. Chem. Soc.* **1992**, *114*, 10146.
(29) Kraitchman, J. *Am. J. Phys.* **1953**, *21*, 17.
(30) Blukis, U.; Kasai, P. H.; Myers, R. J. *J. Chem. Phys.* **1963**, *38*, 2753.
(31) Frisch, M. J.; Trucks, G. W.; Schlegel, H. B.; Scuseria, G. E.; Robb, M. A.; Cheeseman, J. R.; Zakrzewski, V. G.; Montgomery, J. A., Jr.; Stratmann, R. E.; Burant, J. C.; Dapprich, S.; Millam, J. M.; Daniels, A. D.; Kudin, K. N.; Strain, M. C.; Farkas, O.; Tomasi, J.; Barone, V.; Cossi, M.; Cammi, R.; Mennucci, B.; Pomelli, C.; Adamo, C.; Clifford, S.; Ochterski, J.; Petersson, G. A.; Ayala, P. Y.; Cui, Q.; Morokuma, K.; Malick, D. K.; Rabuck, A. D.; Raghavachari, K.; Foresman, J. B.; Cioslowski, J.; Ortiz, J. V.; Stefanov, B. B.; Liu, G.; Liashenko, A.; Piskorz, P.; Komaromi, I.; Gomperts, R.; Martin, R. L.; Fox, D. J.; Keith, T.; Al-Laham, M. A.; Peng, C. Y.; Nanayakkara, A.; Gonzalez, C.; Challacombe, M.; Gill, P. M.

W.; Johnson, B. G.; Chen, W.; Wong, M. W.; Andres, J. L.; Head-Gordon, M.; Replogle, E. S.; Pople, J. A. *Gaussian 98W*, revision A.11; Gaussian, Inc.: Pittsburgh, PA, 1998.

(32) Frisch, M. J.; Trucks, G. W.; Schlegel, H. B.; Scuseria, G. E.; Robb, M. A.; Cheeseman, J. R.; Zakrzewski, V. G.; Montgomery, J. A., Jr.; Stratmann, R. E.; Burant, J. C.; Dapprich, S.; Millam, J. M.; Daniels, A. D.; Kudin, K. N.; Strain, M. C.; Farkas, O.; Tomasi, J.; Barone, V.; Cossi, M.; Cammi, R.; Mennucci, B.; Pomelli, C.; Adamo, C.; Clifford, S.; Ochterski, J.; Petersson, G. A.; Ayala, P. Y.; Cui, Q.; Morokuma, K.; Malick, D. K.; Rabuck, A. D.; Raghavachari, K.; Foresman, J. B.; Cioslowski, J.; Ortiz, J. V.; Baboul, A. G.; Stefanov, B. B.; Liu, G.; Liashenko, A.; Piskorz, P.; Komaromi, I.; Gomperts, R.; Martin, R. L.; Fox, D. J.; Keith, T.; Al-Laham, M. A.; Peng, C. Y.; Nanayakkara, A.; Gonzalez, C.; Challacombe, M.; Gill, P. M. W.; Johnson, B. G.; Chen, W.; Wong, M. W.; Andres, J. L.; Head-Gordon, M.; Replogle, E. S.; Pople, J. A. *Gaussian 98*, revision A.9; Gaussian, Inc.: Pittsburgh, PA, 1998.

(33) Simon, S.; Duran, M.; Dannenberg, J. J. *J. Chem. Phys*. **1996**, *105*, 11024.

(34) Boys, S. F.; Bernardi, F. *Mol. Phys.* **1970**, *19*, 553.

(35) van Duijneveldt, F. B.; van Duijneveldt-van de Rijdt, G. C. M.; van Lenthe, J. H. *Chem. Rev*. **1994**, *94*, 1873.

(36) Turi, L.; Dannenberg, J. J. *J. Phys. Chem*. **1993**, *97*, 7899.

(37) Xantheas, S. S. *J. Chem. Phys*. **1996**, *104*, 8821.

(38) The vibrational modes are labeled using the Herzberg convention for the DME monomer. ν_1 and ν_{12} describe methyl group C−H stretching modes (CH_3 d str, where the d denotes degenerate).